Journal of Building Engineering 25 (2019) 100813

Contents lists available at ScienceDirect

Journal of Building Engineering

journal homepage: www.elsevier.com/locate/jobe

Comparative fragility methods for seismic assessment of masonry buildings located in Muccia (Italy)

Nicola Chieffo[a,*], Francesco Clementi[b], Antonio Formisano[c], Stefano Lenci[b]

[a] Faculty of Architecture and Urbanism, Politehnica University of Timişoara, Romania
[b] Department of Civil and Building Engineering, and Architecture, Polytechnic University of Marche, Italy
[c] Department of Structures for Engineering and Architecture, University of Naples "Federico II", Italy

ARTICLE INFO

Keywords:
Masonry buildings
Empirical method
Mechanical method
Vulnerability assessment
Damage scenarios
Fragility curves

ABSTRACT

The current paper focuses on a sector of the historic centre of Muccia, in the district of Macerata (Italy), affected by the seismic sequence that involved Central Italy in 2016. The main goal is comparison, in terms of fragility curves, among two vulnerability assessment methodologies (empirical and mechanical). The study area has been structurally and typologically identified according to the Building Typology Matrix (BTM). Physical vulnerability analysis of the urban-sector was performed through application of an index-based method, specifically for masonry building aggregates. An isolated masonry building, damaged after the seismic sequences, has been selected as a case study. For the assessed building, empirical fragility curves are presented according to Guagenti & Petrini's correlation law. Furthermore, a numerical model has been set up by using the macro-element approach, which has allowed to perform non-linear static analyses. Mechanical properties of masonry were defined according to the New Technical Codes for Constructions (NTC18), assuming a limited knowledge level (LC1). Refined mechanical fragility functions have been derived and compared to the empirical ones.

Analysis results have shown that the empirical method tends to overestimate by 5% and 10% the expected damage for slight and moderate thresholds. For PGA values greater than 0,3 g the damage levels decreased by 30% and 20%, with reference to the near collapse and collapse conditions, respectively.

1. State of art

The seismic risk assessment is a multivariate problem based on the estimation of three major factors such as vulnerability (V), exposure (E), and hazard (H). The combination of these factors allows to qualitatively and quantitatively describe the risk in a given region as a result of catastrophic events. The estimation of these three factors is very important for an appropriate preventive analysis oriented towards the seismic risk assessment of urban areas in order to plan reasonable interventions for risk mitigation [1,2]. The concept of vulnerability, V, is mainly based on the capacity of a class of buildings to suffer specific damage due to a seismic event. The exposure, E, is connected to the nature, quantity, and value of the properties and activities of the area that can be influenced directly or indirectly by a seismic event. Finally, the hazard, H, can be understood as the probability of occurrence of an event in a specific site and depends mainly on the both, geographic position and geological characteristics of the area. The seismic hazard is defined as the probability of exceeds an intensity measurement (*IM*) in a specific seismogenic area.

Masonry has been one of the most popular construction materials developed during the centuries as it provided economic and functional solutions worldwide. Nevertheless, the existing unreinforced masonry buildings (URM) are typically identified as "potential risk factors" due to the behavior of masonry that is very complicated to be predicted. In fact, when the URM buildings are subjected to shaking due to the earthquake, the mass of the walls and lightweight flexible diaphragms leads to a rigid-fragile global behavior that triggers the possible collapse mechanisms increasing the possibility of repercussions on society (physical and economic losses). Generally, these constructions have been designed to resist only gravity loads, offering very low resistance to seismic actions [3,4].

The URM response depends on many aspects that affect mainly the ductility of the piers and strength of the walls [5]. The failure mode is affected by several parameters, such as the vertical compression due to gravity loads, the wall aspect ratio, the boundary conditions, and the relative strength between mortar joints and units. In the past, strong

* Corresponding author. Politehnica University of Timisoara, Faculty of Architecture and Urbanism, 2/A Traian Lalescu street, 300223, Timisoara, Romania.
E-mail addresses: nicola.chieffo@student.upt.ro (N. Chieffo), francesco.clementi@univpm.it (F. Clementi), antoform@unina.it (A. Formisano), lenci@univpm.it (S. Lenci).

https://doi.org/10.1016/j.jobe.2019.100813
Received 19 April 2019; Received in revised form 27 May 2019; Accepted 30 May 2019
Available online 06 June 2019

earthquakes have caused considerable damage given the poor consistency of the building samples. The damage is attributed to inadequate structural integrity and to the lack of connection between the orthogonal walls which results in typical shear cracking and disintegration of the walls with consequent partial or total collapses [6,7]. It seems evident that the many uncertainties, mainly associated with the mechanical characteristics of the basic material (not homogeneous and anisotropic) and construction techniques, negatively influence the structures' capacity to overcome a seismic event [8].

Focusing on historical centers, they are characterised by numerous buildings of immeasurable architectural and cultural value.

In fact, the large number of old masonry buildings in many of the Italian seismic areas represents one of the crucial points for the preservation and protection of the existing heritage.

The heterogeneity of buildings placed in aggregate is a very delicate aspect since it requires a significant level of knowledge on every single structural unit (S.U.). Nevertheless, ordinary buildings located in the historical centers are often made of different quality of masonries and constructive details that can highlight deficiencies with respect to safety conditions against seismic actions [9,10]. A significant number of proposals based on simplified modeling approaches is already available in the scientific literature. Most of them are based on the assumption that the masonry wall is represented as a set of one-dimensional macro-elements (piers and spandrels), connected by nodes in such a way as to reproduce the behavior of the wall by an equivalent frame, which gives the possibility of using conventional numerical methods of structural mechanics [11,12]. Other advanced methods, proposed in Refs. [13,14], investigates the seismic response by means of non-linear dynamic analysis on 3D FEM model, assuming that masonry behaves as a damaging-plastic material with almost vanishing tensile strength. Generally, the presence of vulnerability factors is a fundamental feature that significantly decreases the strength of the walls, influencing the damage distribution mainly due to out-of-plane actions. Furthermore, it has been stated that a preliminary structural assessment through kinematic limit analysis on partial failure mechanisms may be reliable only after a proper estimation of the different structural elements playing a role in the horizontal behavior (e.g. interlocking between walls, typology of masonry, distribution of horizontal loads, constraints and dead loads distribution, etc.). The comparison between the numerical results and the damage survey showed that the numerical approach used in Ref. [15] may be an adequate tool to properly evaluate the seismic response of historical masonry buildings. However, it would be unreasonable to perform numerical analyses on each individual building within historic centers.

To this purpose, the large-scale evaluation methodologies are mainly based on observational data for a significant sample of buildings, therefore, for the evaluation of the seismic vulnerability of the aggregates, rapid approaches are generally used (vulnerability index method) for an appropriate vulnerability estimate and the attribution of the vulnerability class is supported on information on buildings (drawings and on-site inspections) [16,17]. The peculiarity of this methodology is the possibility of combining it with the macroseismic method for the assessment of damage scenarios. The macroseismic methodology, therefore, allows evaluating the susceptibility to damage of a stock of buildings, varying the level of the expected hazard which is defined as macroseismic intensity according to EMS-98 scale [18]. The possibility of identifying the most vulnerable sample of buildings allows previously to mitigate the effects of the seismic phenomenon [19].

Based on these premises, the main goal of this research work is to identify the seismic response of an isolated masonry building by means of fragility curves developed using different vulnerability assessment methodologies.

2. Historical background of the city of Muccia

The City of Muccia (Fig. 1) is an Italian town of 911 inhabitants in the province of Macerata in the Marche region. The Municipality is 454 m on the sea level with an area of 25.91 Km^2. On the banks of the Chienti River, located at an important road junction since antiquity, Muccia hosts numerous archeological finds, remarkable 15th-century churches and a wonderful Franciscan hermitage, oasis of peace and meditation. Since prehistory, has been characterised as a knot of important communication channels. In the middle Ages, under the name of Mutia, it was a strategic place for the processing and trade of grains, so that the lordship of Da Varano di Camerino erected a castle in defense of mills [20].

On January 1436 it was sacked by the troops of Francesco Sforza when he occupied the Marche. His proximity to Camerino makes him presumptuous. Next, with the Napoleonic Kingdom of Italy, was part of the department of Tronto, district of Camerino, canton of the same name.

The advent of the Unity of Italy, the Municipality became part of the province of Macerata in Camerino's mandate. Muccia is also a centre characterised by numerous archeological finds and sites of interest, among which are the Church of Santa Maria di Varano, with an octagonal plan, the "Tower of Massa", "Torraccia" at Mentori a.s.l. 808 m at Massaprofoglio (Fig. 2).

2.1. The central Italy seismic sequences

The first main-shock occurred August 24th, 2016 had its epicenter in the province of Rieti (near the municipality of Accumoli), but it also affected the provinces of Perugia, Ascoli Piceno, L'Aquila and Teramo. The municipalities closest to the epicenter are: Accumoli, Amatrice, Arquata del Tronto. The maximum moment magnitude recorded, M_w, was equal to 6,0. The area affected by the aftershocks, which in a first approximation represents the extension of the activated fault, is approximately 25 km and is aligned in the sense NNO - SSE. Subsequently, several aftershocks have been recorded, the largest of which is in the area of Norcia (PG) with magnitude equal to 5,4. The hypocenter depths of the replicas are modest, almost all within the first 10 km [21].

Two powerful replicas took place on October 26th, 2016 with epicentres at the Umbria-Marche border between the municipalities of Visso, Ussita and Castelsantangelo sul Nera with a magnitude of 5,9. On October 30th, 2016, the strongest shock, magnitude 6,5, with the epicenter between the municipalities of Norcia and Preci, in the Province of Perugia was recorded.

The observations and preliminary analyses prepared by INGV [22] through seismological surveys, allowed a first interpretation of the event (Fig. 3).

The seismogenetic area was characterised by the presence of different segments of fault with high structural complexity.

The focal mechanisms (*slip*) allow identifying the type of movement that occurred following a specific earthquake, then how the area moved in response to tectonic deformation as reported in Fig. 4.

Already from the morning of August 24th, following the first excavations in the area, some surface fractures (cosmic effects) have been discovered and mapped [23], showing continuity of at least 1,8 km from the Monte Vettore side. The maximum of cosismic deformation seems to be found near Accumoli (Fig. 5).

The area was characterised by a vertical extension indicated with "+" in the previous figure, while, the zone subject to a depression, is indicated with the symbol "-". The green line indicates the seismic fault that generated the earthquake.

3. Seismic vulnerability assessment of the historical centre of Muccia

3.1. Characterisation of the study area

The sub-urban sector analysed (Fig. 6) is to be considered homogeneous from a typological and structural point of view. It consists of 50

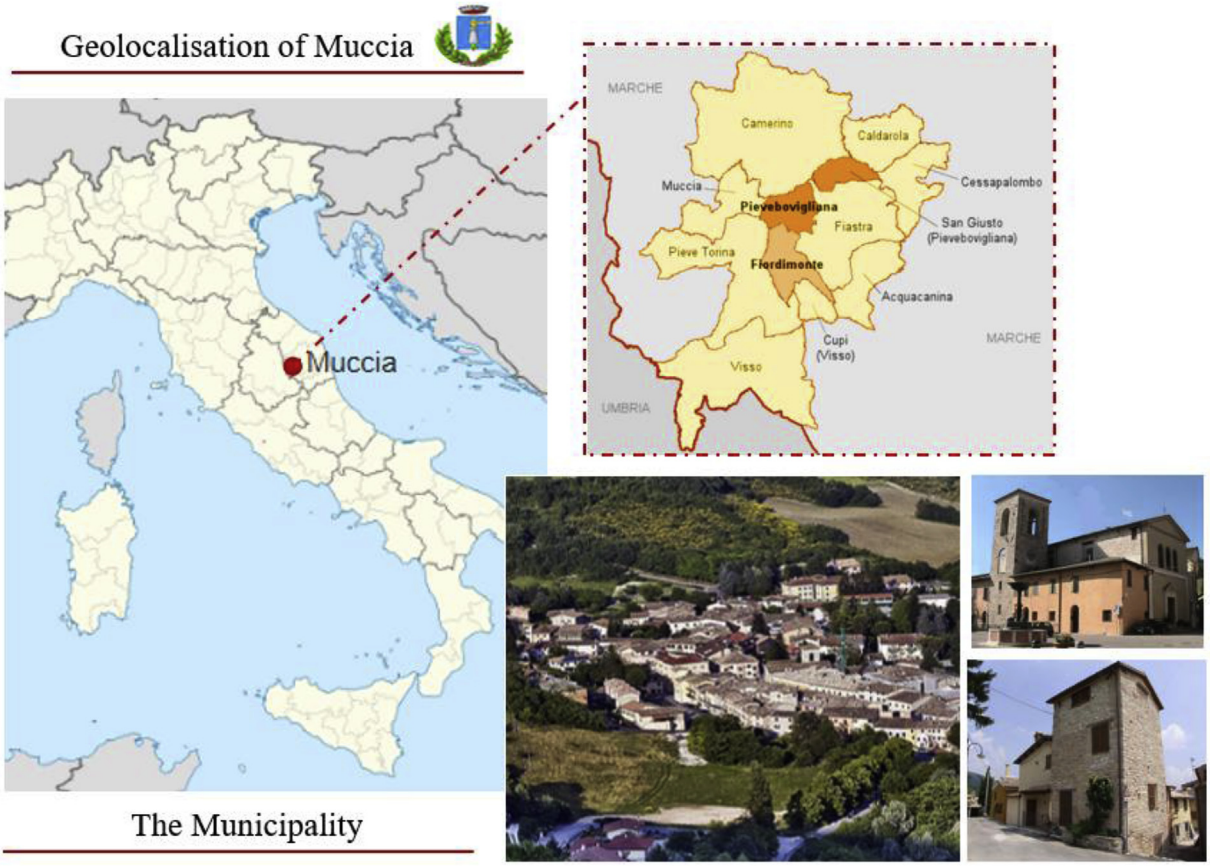

Fig. 1. The city of Muccia in the Marche region of Italy.

masonry structural units (S.U.) dating back to the 19th century.

According to Building Typology Matrix (BTM) [24], this sector is composed of 50 buildings: M3.1 class masonry structures with steel floors (36% of the cases) and M3.3 class masonry structures with wooden floors (54%) and M3.4 masonry structures with rc floors (10%) (Fig. 7).

The masonry aggregates are generally developed in elevation from 2 to 3 stories. The inter-storey height is about 3,00–4,00 m for the first level and 3,00–3,50 m for other floors.

Roofing structures are often composed of double pitch r.c. beams with clay tile covering or wooden elements. In many cases, the presence in the walls of an incongruous and brittle binder, which lost over time its characteristics, compromises the static nature of the buildings themselves and, sometimes, of the whole aggregate. The presence of these vulnerability factors increases the possibility of collapse and instability of the historical built-up when subjected to an impacting seismic action (Fig. 8).

3.2. Seismic vulnerability assessment

Aiming at implementing a quick seismic evaluation procedure for masonry aggregates, it has been used the new vulnerability form proposed in Table 1 [25], which has been used in recent years for the seismic vulnerability assessment of several historical masonry aggregates [26,27] (Table 1).

This new form is based on the method of the vulnerability index devised by Benedetti and Petrini [28]. This survey form is composed of 10 basic parameters and has been widely used in the past to survey the main structural system and the fundamental seismic deficiencies of isolated buildings in the case of an earthquake. In order to consider the

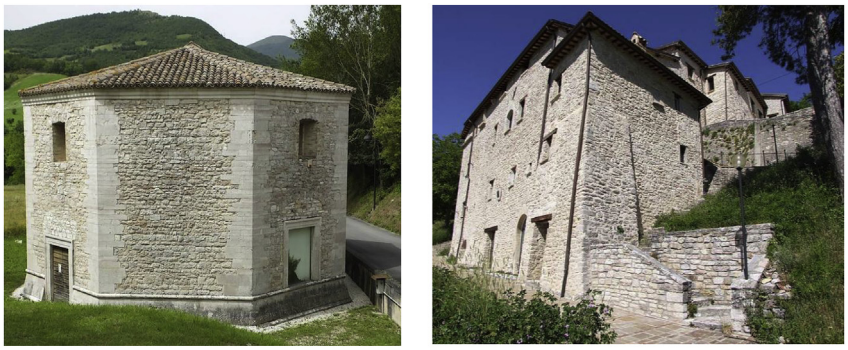

(a) (b)

Fig. 2. Archeological site: a) Sant Maria di Varano Church; b) Massaproglio Castle.

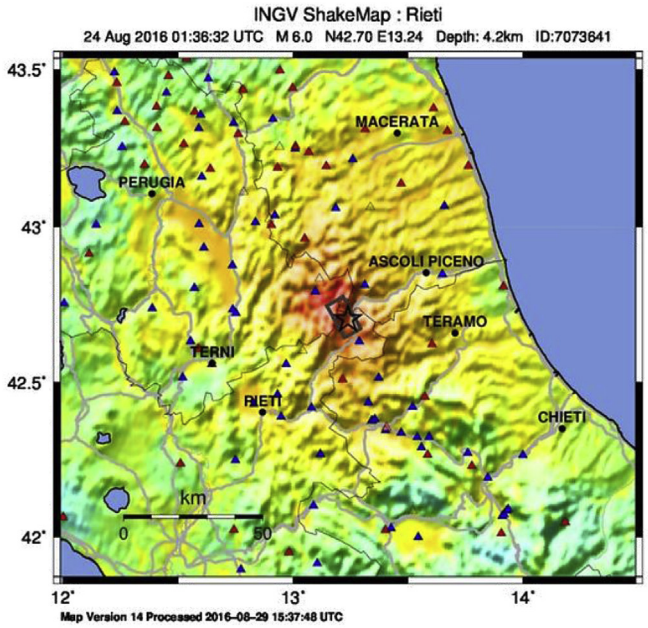

(a)

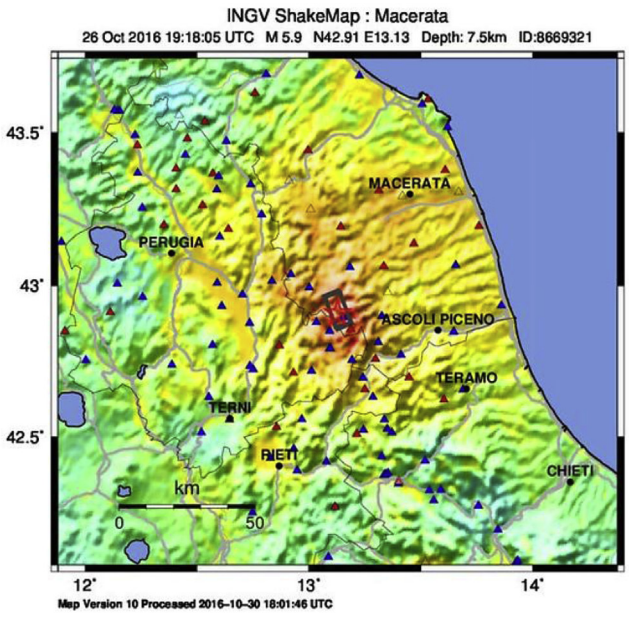

(b)

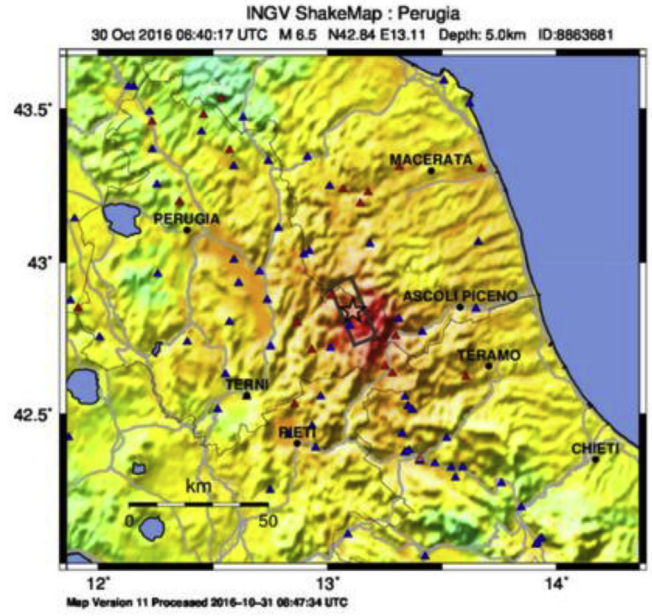

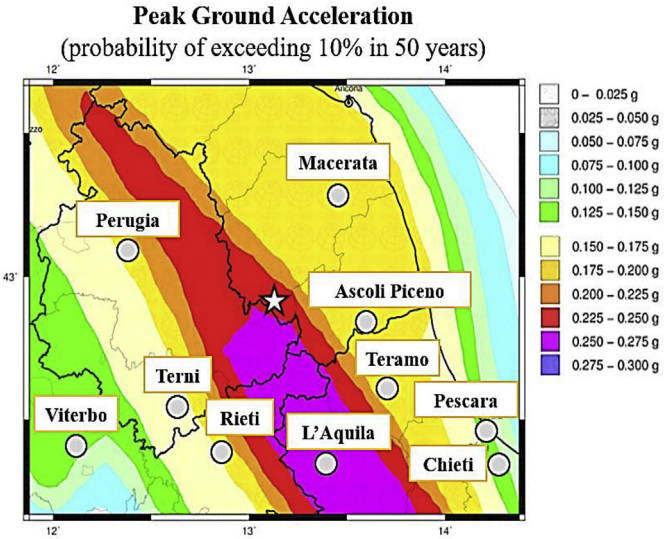

PERCEIVED SHAKING	Not felt	Weak	Light	Moderate	Strong	Very strong	Severe	Violent	Extreme
POTENTIAL DAMAGE	none	none	none	Very light	Light	Moderate	Mod./Heavy	Heavy	Very Heavy
PEAK ACC.(%g)	<0.06	0.2	0.8	2.0	4.8	12	29	70	>171
PEAK VEL.(cm/s)	*<0.02*	*0.08*	*0.3*	*0.9*	*2.4*	*6.4*	*17*	*45*	*>120*
INSTRUMENTAL INTENSITY	I	II–III	IV	V	VI	VII	VIII	IX	X+

Scale based upon Faenza and Michelini, 2010, 2011

(c)

Fig. 3. Shakemaps of the events occurred: (a) August 24th, 2016; (b) October 26th, 2016 and (c) October 30th, 2016 [22].

structural interaction between adjacent buildings, not considered in the previously mentioned method, a new form has been adopted. The new form of investigation, appropriately conceived for the aggregates of masonry buildings, is conceived by adding five new parameters to the ten basic parameters of the original form. These new parameters take into account the interaction effects between the aggregate structural units under earthquake [29]. The added parameters, partially derived from previous studies are:

– Parameter 11: Presence of adjacent buildings with different height.

1 The elevation interaction among adjacent buildings takes into account the different height of the adjacent buildings. S.U. placed between buildings with the same height or higher are generally the

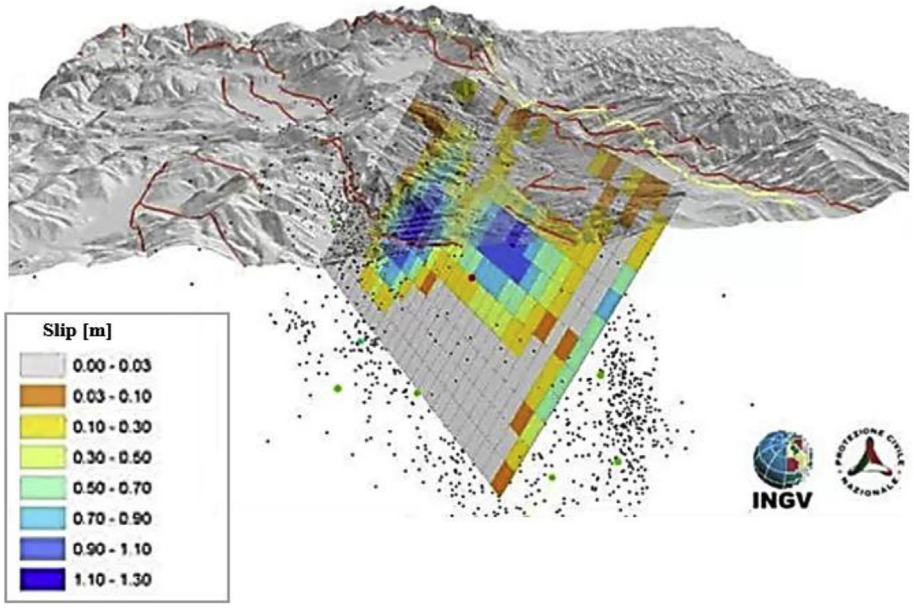

Fig. 4. The focal mechanism occurred [22].

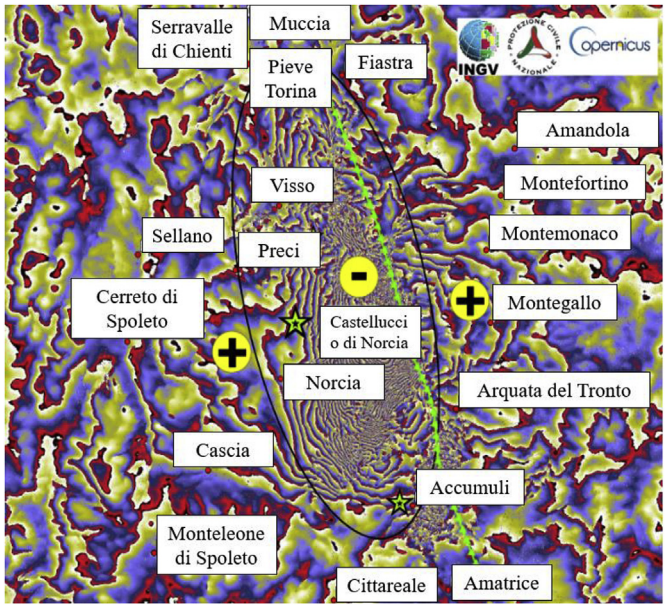

Fig. 5. The coseismic deformation map [23].

Fig. 6. The sub-urban sector identification.

least vulnerable constructions.

2 On the contrary, the most unfavourable cases are when S.U. is located between two lower buildings (one and two floors). In these cases, since the binding action of the adjacent buildings is only partial, the central building is free to deform laterally to the last levels with the possibility of triggering out-of-plane mechanisms.

– Parameter 12: Position of the building in the aggregate.

3 This parameter provides indications about the in-plane interaction among S.U. In particular, this parameter allows to distinguish different positions and, consequently, different structural behaviours of S.U. in the aggregate. Four possible positions are considered: isolated, enclosed between buildings, in a corner position, and in heading position. It is worth noting that the inclusion in aggregate, regardless of the position of the structural unit, always gives rise to the reduction of seismic vulnerability.

– Parameter 13: Number of staggered floors.

4 The presence of staggered floors is contemplated for the pounding effects among adjacent S.U., since different heights of the buildings could activate out-of-plane mechanisms.

– Parameter 14: Structural or typological heterogeneity among adjacent S.U.

5 This parameter accounts for the structural or typological heterogeneity among adjacent S.U. According to the formulation adopted, the building aggregates can be considered homogeneous (from the typological and structural point of view) when they present the same material and the same construction technique, which is the most favourable case.

– Parameter 15: Percentage difference of opening areas among adjacent facades.

6 This parameter takes into account the distribution of horizontal actions among façades of adjacent buildings. This factor influences negatively the seismic response of the façade. Actually, the larger the percentage of openings difference between two adjacent facades,

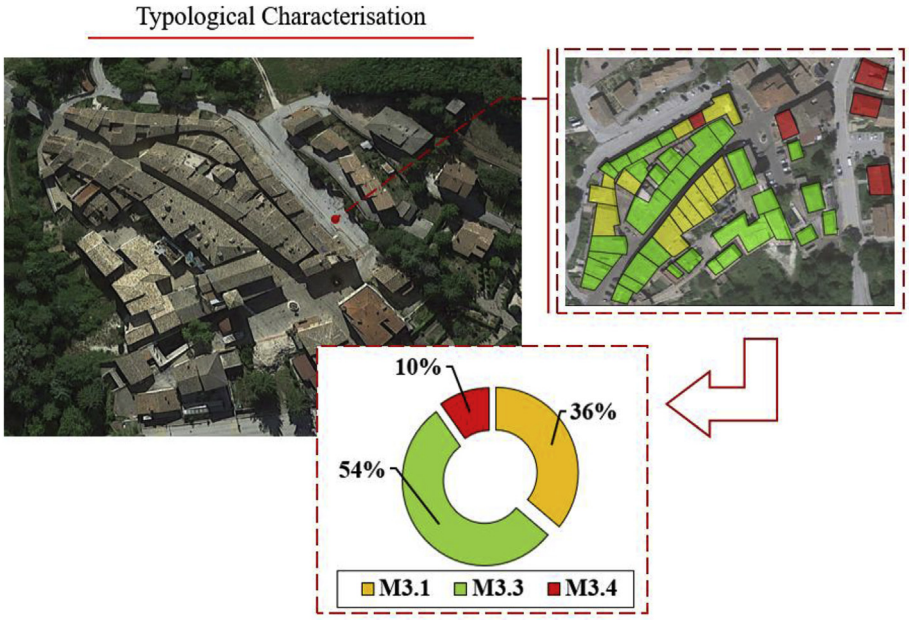

Fig. 7. Typological characterisation of the sub-urban sector.

Fig. 8. Building conformation: a) vertical configuration; b) structural heterogeneities.

Table 1
The vulnerability form for buildings in aggregate.

Parameters	Class Score, S_i				Weight, W_i
	A	B	C	D	
1. Organization of vertical structures	0	5	20	45	1,00
2. Nature of vertical structures	0	5	25	45	0,25
3. Location of the building and type of foundation	0	5	25	45	0,75
4. Distribution of plan resisting elements	0	5	25	45	1,50
5. In-plane regularity	0	5	25	45	0,50
6. Vertical regularity	0	5	25	45	0,50
7. Type of floor	0	5	15	45	0,80
8. Roofing	0	15	25	45	0,75
9. Details	0	0	25	45	0,25
10. Physical conditions	0	5	25	45	1,00
11. Presence of adjacent building with different height	−20	0	15	45	1,00
12. Position of the building in the aggregate	−45	−25	−15	0	1,50
13. Number of staggered floors	0	15	25	45	0,50
14. Structural or typological heterogeneity among adjacent S.U.	−15	−10	0	45	1,20
15. Percentage difference of opening areas among adjacent facades	−20	0	25	45	1,00

the worse the distribution of horizontal loads between them.

Formally, the methodology is based on the evaluation of a vulnerability index, I_v, for each S.U. of the aggregate intended as the weighted sum of the 15 parameters mentioned above.

In Table 1, it is possible to notice how these parameters are distributed into four classes (A, B, C and D) with scores, S_i, of growing vulnerability.

A weight, W_i, is associated with each parameter that can range from 0,25 for the less important parameters to a maximum of 1,50 for the most important ones. According to this, the vulnerability index, I_v, can be calculated according to the following equation:

$$I_V = \sum_{i=1}^{15} S_i \times W_i \tag{1}$$

Subsequently, I_v is normalised in the range [0 ÷ 1], adopting the notation V_I, by means of the following relationship:

$$V_I = \left[\frac{I_V - (\sum_{i=1}^{15} S_{\min} \times W_i)}{|\sum_{i=1}^{15} [(S_{\max} \times W_i) - (S_{\min} \times W_i)]|} \right] \tag{2}$$

Based on these premises, the statistical distributions of the global vulnerability of the sub-urban sector analysed has been depicted in Fig. 9.

From the analysis of results, it is worth noting how 28% of the building classes M3.1 have a vulnerability index of 0,42 and only 5%

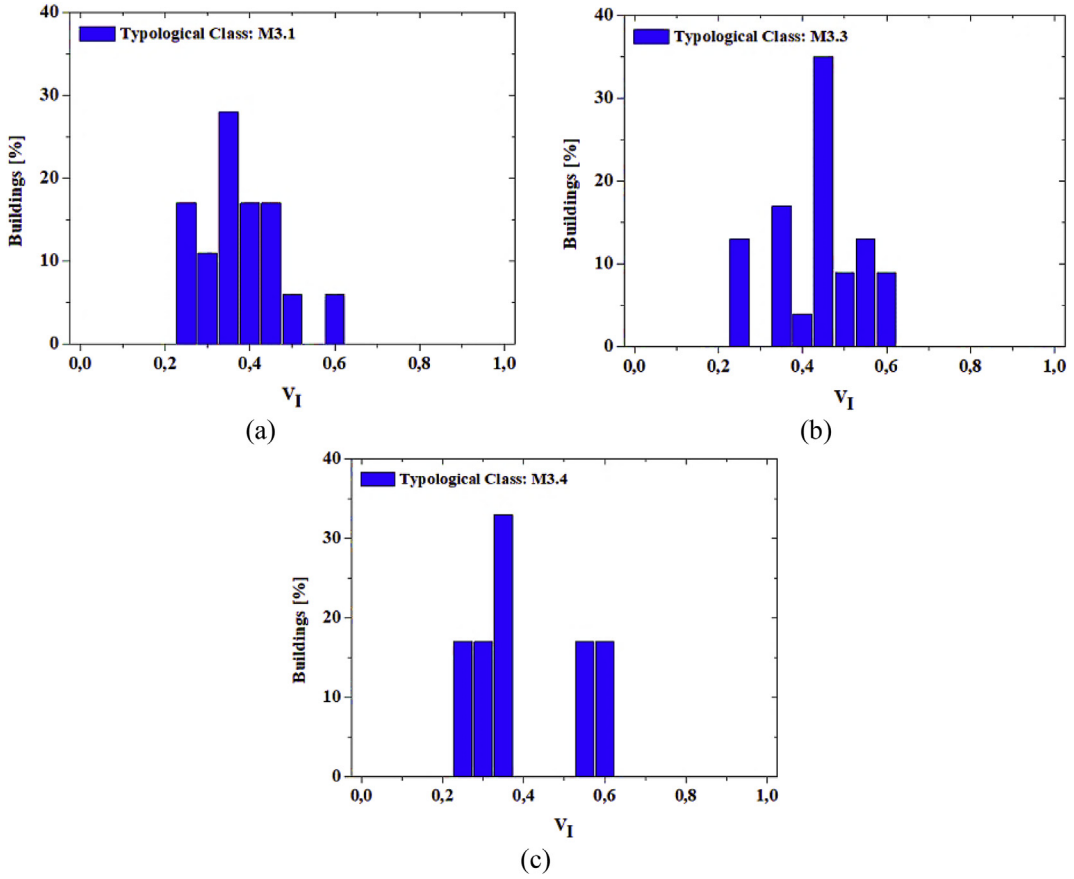

Fig. 9. Vulnerability frequency distributions of the sample of buildings belonging to (a) M3.1, (b) M3.3 and (c) M3.4 typological classes.

have indexes of 0,50 and 0,60, respectively. Similarly, for the class M3.3, 34% of the cases have a vulnerability index of 0,42 and only 3% provides an index of 0,38. Finally, considering the M3.4 class, 35% of the sample have an index of 0,38 and only 15% have indexes of 0,20 and 0,60, respectively.

3.3. Typological vulnerability curves

The proposed procedure, developed by Ref. [30], allows correlated macroseismic intensity, according to the EMS-98 scale, with the expected mean damage grade mathematically expressed by Eq. (3).

$$\mu_D = 2{,}5\left[1 + \tanh\left(\frac{I + 6{,}25 \times V_I - 13{,}1}{Q}\right)\right] \quad (3)$$

As can be seen, the vulnerability curves depend on three variables: the normalised vulnerability index (V_I), the hazard, expressed in terms of macroseismic intensity (I), and a ductility factor Q, ranging from 1 to 4, which describes the ductility of typological classes of buildings and has been assumed as equal to 2,3 [30]. Therefore, the mean vulnerability curves shown in Fig. 10 have been plotted in order to estimate the collapse probability of analysed buildings for different scenarios (V_I-$\sigma_{VI,\ Mean}$; $V_I + \sigma_{VI,\ Mean}$; $VI + 2\sigma_{VI,\ Mean;\ VI} + 2\sigma_{VI,\ Mean}$) [31,32].

4. Estimated damage scenario

4.1. Damage model prediction

Scenario analysis allows to investigate the damage associated with a generic structural system when subjected to a natural event. Referring to the examined case study, and according to Section 2.1, a set of magnitudes, enclosed in the range [5,4–6,5] have been selected.

The severity of the damage was analysed by means of a predictive analysis in which, during the earthquake, buildings with the same structural characteristics would be subject to damage that decreases when increasing the epicentral distance. Subsequently, the attenuation law proposed by by Crespellani [33] has been used in order to characterise the seismic scenario and reported in Equation (4).

$$I_{EMS-98} = 6{,}39 + 1{,}756M_w - 2{,}747 \times \ln(R + 7) \quad (4)$$

where M_w is the moment magnitude occurred and R is the site-source distance expressed in Km.

According to the scale EMS-98, six damage levels, D_k, each one associated to a damage score k, ranging from 0 to 5, are defined: *D0:* no damage; *D1(moderate damage)*: with hair-line cracks in very few walls and fall of small pieces of plaster only; *D2 (substantial damage)*: structural damage and moderate non-structural damage. Cracks in many walls with fall of fairly large pieces of plaster. Partial collapse of chimneys; *D3 (significant damage):* intensive structural damage and heavy non-structural damage, with large and extensive cracks in most walls; roof tiles detachment; chimneys fracture at the roofline; failure of individual non-structural elements (partitions, gable walls); activation of the first out-of-plane mechanisms; *D4 (partial collapse):* extended damage and very heavy non-structural damage, with serious wall failures; partial structural failure of roofs and floors; *D5 (collapse):* collapse to both non-structural and structural parts, with total or near total collapse of the whole building. Considering the representative damage parameter μ_D, the expected number of buildings that undergo a certain damage level has been determined (Fig. 11).

A complete damage distribution has been defined from the scenario previously achieved. The conditional probability, $P[D_k > D_i|M_w; R]$, of exceeding a certain damage state, D_k, varying the magnitude, M_w, and epicentral distances, R were presented in Fig. 12.

As can be seen, for a moment magnitude, M_w, equal to 5,4, 100% of

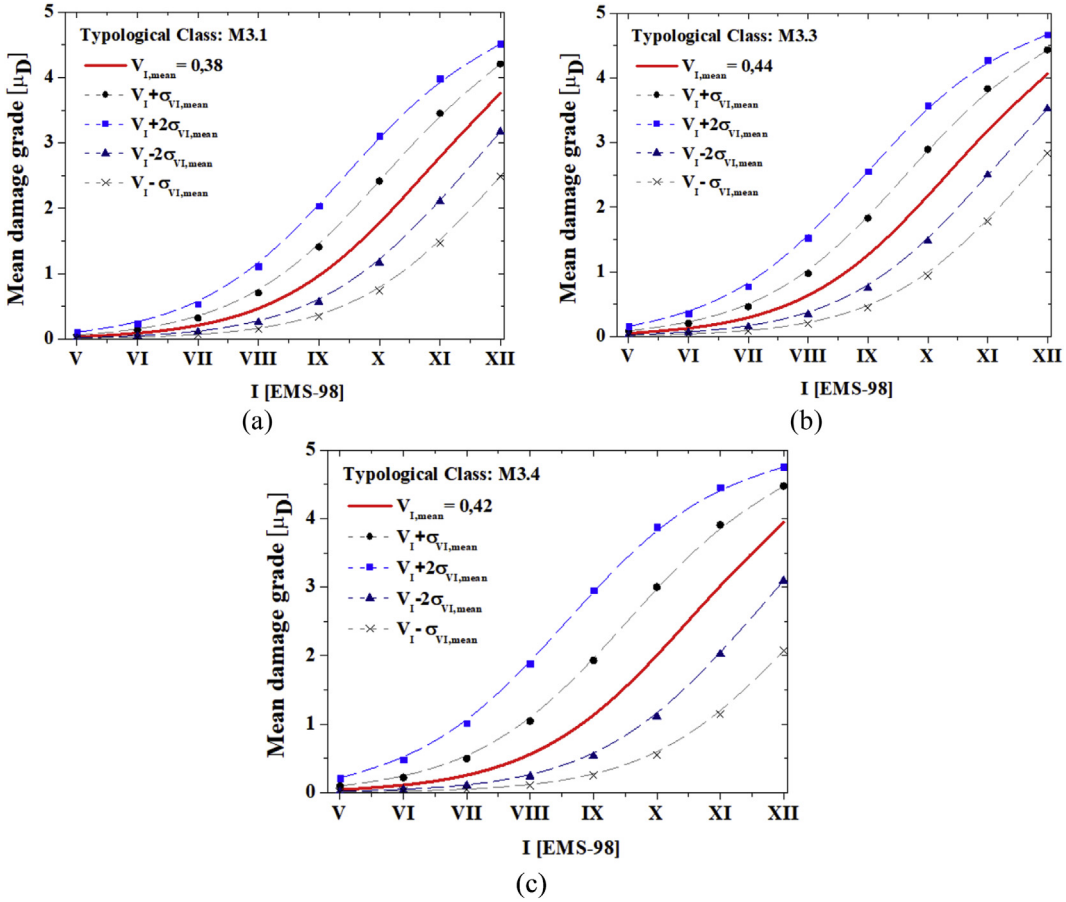

Fig. 10. Mean typological vulnerability curves for the sample of buildings examinated.

building stocks reached damage D0 (No Damage). Consequently, for a magnitude 6,0, the damage distribution has shown that 90% of the cases reached damage D0, whereas only 10% of the sample are characterised by damage D2. Furthermore, referring to the event occurred on October 30th (epicenter localized in Accumuli), for a moment magnitude equal to 6,5, the damage distribution provided 40% of the building's cases suffered D2 damage (Substantial damage), 6% suffered a damage D3 and only 8% of the buildings sample have D4 damage (Extended damage).

Moreover, considering the event occurred on October 30th, the correlation among empirical damage scenario and site-inspection recognition have been shown in Fig. 13.

4.2. Empirical fragility curves

Once the global vulnerability of the examined sub-sector was achieved, it was possible to focus attention on the case study building indicated with the number 45 in the previous Section 3. The isolated building examined is reported in Fig. 14. It is characterised by load-bearing masonry walls, with wooden floors and pitched roofs with an average height of 3,50 m.

The physical conditions denote widespread damage characterised by the presence of cracks along the West and North façades, respectively.

The vulnerability index, V_I, derived from the index-based method for isolated buildings, is equal to 0,40. Fragility curves are used to

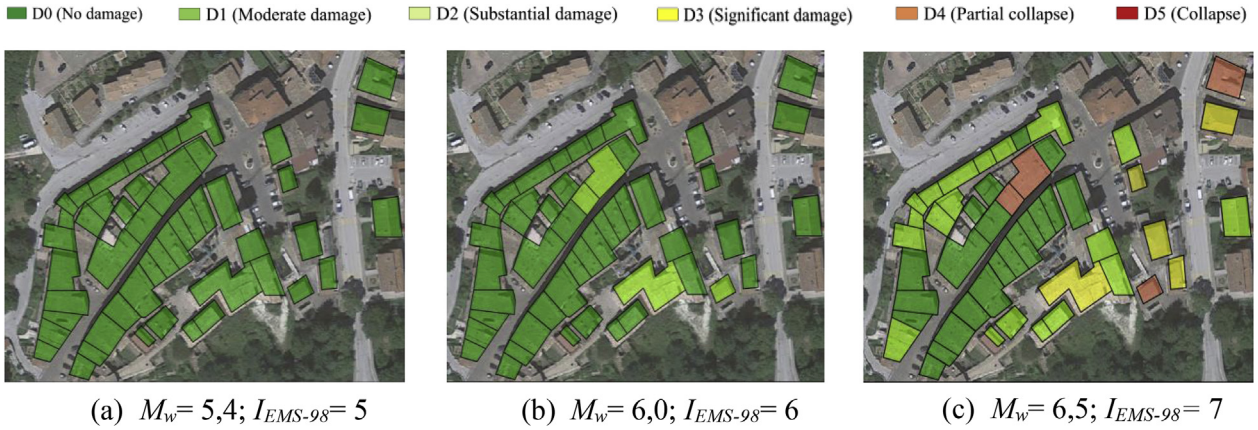

Fig. 11. Damage scenarios for a set of moment magnitudes occurred.

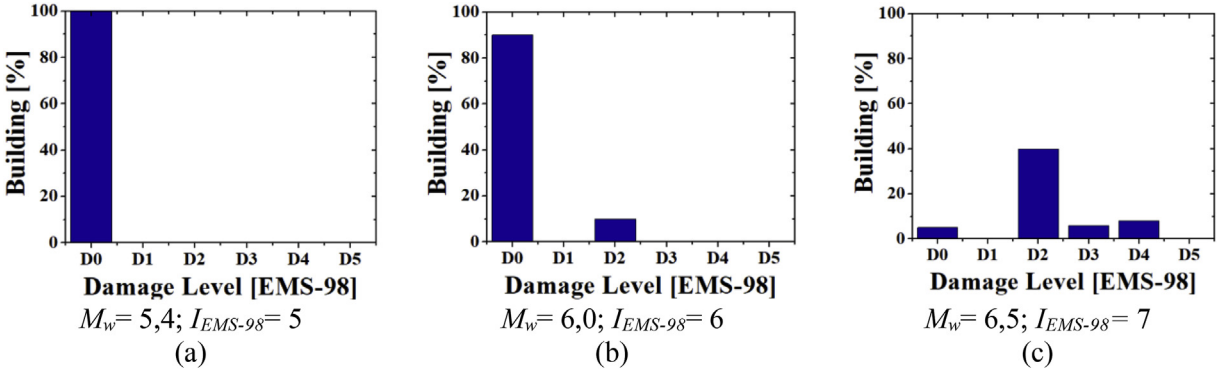

Fig. 12. Vulnerability frequency distributions: (a) M3.1, (b) M3.3 and (c) M3.4 typological classes.

define the probability of exceeding damage threshold, D_k ($K \in [0 \div 5]$). To this purpose, a correlation law, proposed by Gaugenti-Petrini [34], is adopted in Equation (5).

$$\ln(PGA) = 0{,}602I - 7{,}073 \quad [g] \tag{5}$$

Mathematically, this law provides the variation of PGA as a function of macroseismic intensity, I, through empirical correlation coefficients C_1 (0,602) and C_2 (7073). The gotten results are plotted in Fig. 15.

5. Mechanical vulnerability approach

5.1. Assessment of the structural properties

The mechanical characteristics of the materials were chosen according to Italian New Technical Codes for Constructions (NTC18) [35]. The masonry walls, both perimeter and internal, assume a constant thickness in elevation, without the presence of diffused heterogeneity. The mean compressive strength of masonry (f_m) and shear strength (τ_0) are to be considered as minimum values of the range established by NTC18 referring to existing masonry buildings, respectively of 1,00 N/mm^2 and 0,02 N/mm^2. The modulus of elasticity, E, have been considered of 870 N/mm^2, as well as the tangential shear modulus, G, equal to 290 N/mm^2. The specific weight of the masonry, W, is equal to 19,37 kN/m^3 as listed in Table 2. Moreover, the mechanical properties of the timber elements (oak) are given in Table 3. The expected level of knowledge adopted is LC1 which corresponds to a reduction factor of the mechanical properties of the materials, F.C, equal to 1,35.

5.2. Non-linear static analysis

Non-linear static analysis has been performed by using 3Muri software developed by S.T.A. DATA srl [36]. From a geometric point of view, the structure consists of masonry walls of 0,60 m with wooden floors (thickness of 0,20 m) and high of 3,50 m at each level.

Concerning the structural models, the structure is schematised through a series of macroelements interconnected to each other, in some cases leading towards the definition of the so-called "equivalent frame" [37–40].

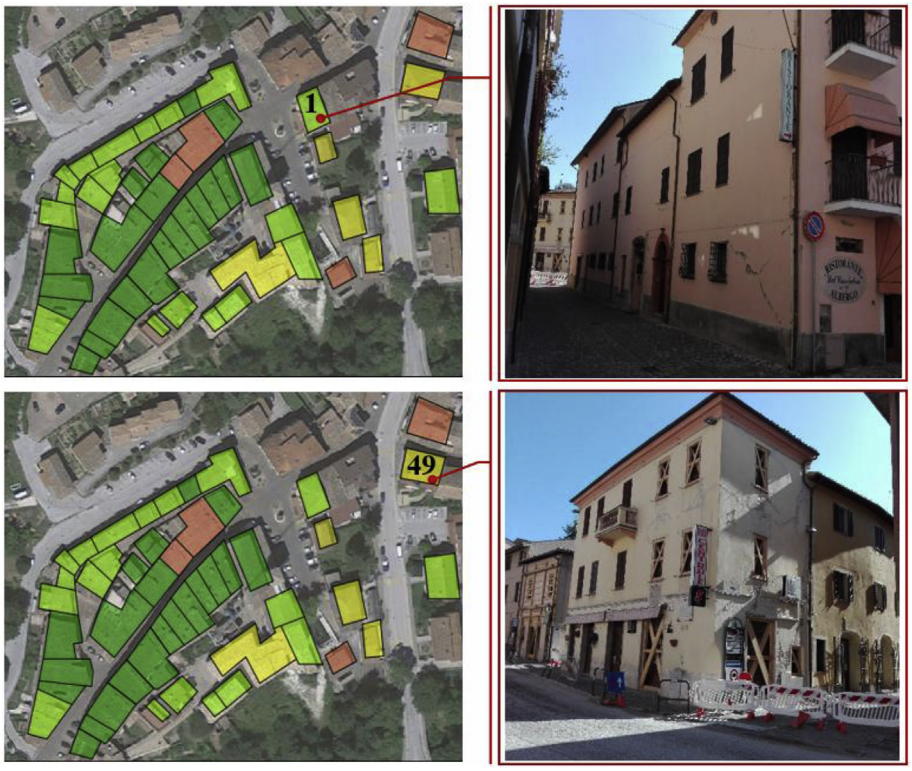

Fig. 13. Correlation among analysed damage scenario and site-inspection.

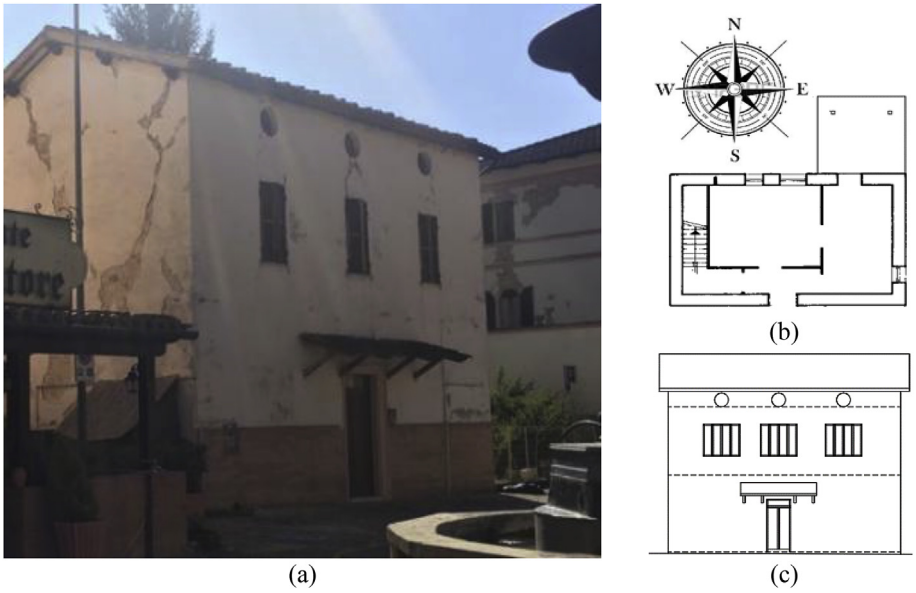

Fig. 14. The case study building n.45, (a) street view, intermediate floor (b) and (c) North prospect.

These macro-elements aim at simulating the seismic behavior of masonry structures, providing all the information required for their static linear analyses.

The 3Muri software uses macro-elements to generate the 3D model of the structure, which is then automatically transformed into an assemblage of 3D equivalent frames to perform pushover analyses. The typical macro-element used for static linear analyses is schematised with the kinematic model reported in Fig. 16 (a). The 3D model of the examined housing building, where it is apparent that masonry walls are modelled through a mesh of masonry piers and spandrels, is depicted in Fig. 16 (b).

The resistance criteria are given on the basis of EN 1998-3 [41] according to which the drift for shear and flexural crack mechanisms are established equal to 0,4% and 0,8% of the ultimate displacement (d_u). The shear capacity model is based on the diagonal cracks model according to the Italian seismic code, NTC18 [35]. The flexural response is developed by neglecting the tensile strength of the material and assuming a uniformly distributed compression stress distribution at the masonry interface.

Numerical analysis was performed considering a soil category "C" and a design spectrum referred to the Life Safety limit state. Dead and variable loads applied at the different structural levels, as well as partial safety factors for gravity loads combination at the Ultimate Limit State, are given in Table 4.

Table 2
Mechanical properties of masonry.

Mechanical Properties	Units	Masonry
Modulus of elasticity	E (N/mm^2)	870
Shear modulus	G (N/mm^2)	290
Mean compressive strenght	f_m (N/mm^2)	1,00
Tensile strength	τ_0 (N/mm^2)	0,02
Specific weight	W (Kg/m^3)	1937

Table 3
Mechanical properties of wooden elements.

Mechanical Properties	Units	Timber
Modulus of elasticity	E (N/mm^2)	800
Shear modulus	G (N/mm^2)	590
Mean compressive strength	f_m (N/mm^2)	18
Tensile strength	τ_0 (N/mm^2)	3,5
Specific weight	W (Kg/m^3)	570

Non-linear static analysis has been performed in the two main directions (X and Y), taking also into account the effect of accidental eccentricities. The analysis results in terms of SDoF capacity curves and corresponding damage level reached in the structure are shown in

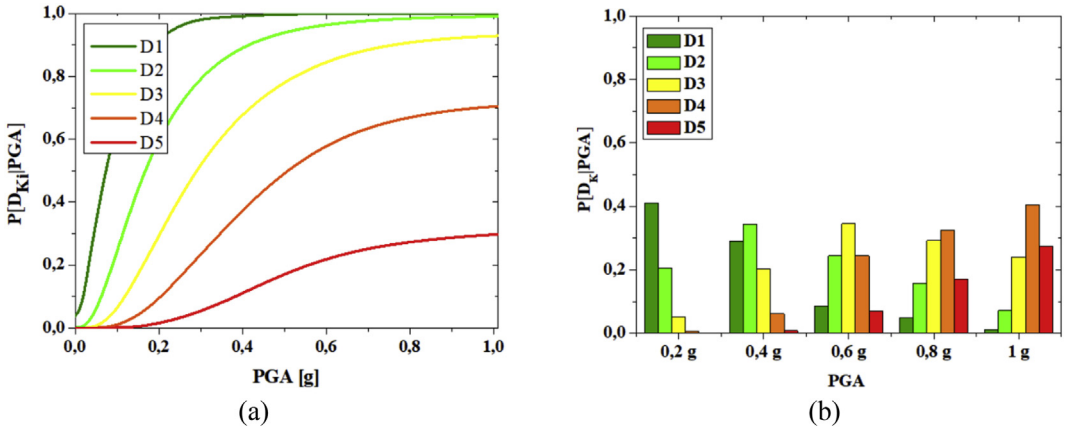

Fig. 15. Fragility curves derived by empirical method (a) and damage distribution (b).

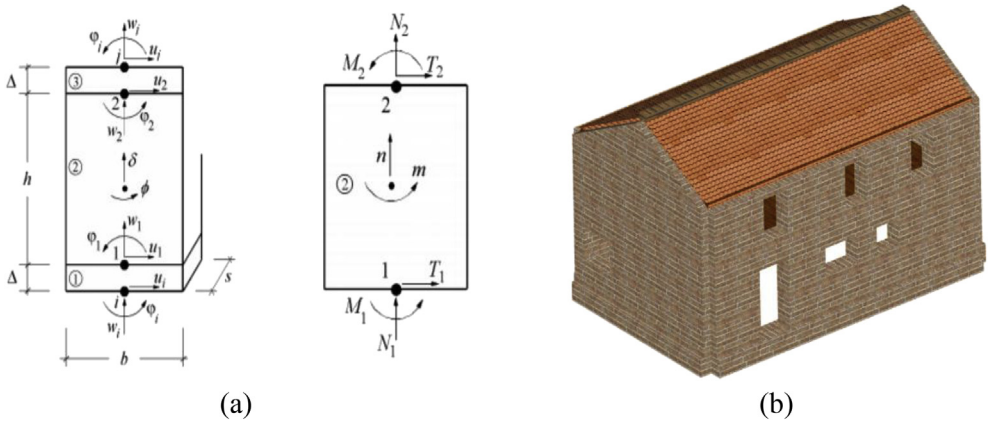

Fig. 16. The macro-element kinematic model (a) and (b) the 3D building model with macro-elements through the 3Muri software.

Table 4
Design load applied.

Static Load	Intermediate Floor [KN/m^2]	Roof [KN/m^2]	Partial safety factor
G_1	3	3	1,3
G_2	2	1	1,3
Q_k	2	0,5	1,5

Fig. 17.

The capacity curves have shown that in *X* direction the structure presents a maximum shear force equal to 272,66 KN with a yielding and ultimate displacements, D_y^* and D_u^*, equal to 0,0029 m and 0,0064 m, respectively. Similarly, in *Y* direction, the maximum shear threshold reached is 360,81 KN to which correspond $D_y^* = 0{,}0030$ m and $D_u^* = 0{,}0065$ m.

Referring to a failure hierarchy, in *X* direction the distribution of ductile mechanisms (bending damage) occurs only in some masonry spandrels, whereas the fragile failures, induced by shear, are reached in the East and West façades, respectively. Moreover, tensile failures are widespread (Fig. 17 (c)). As can be seen, in *Y* direction, the damage tends to increase globally. In fact, in Fig. 17 (d), bending failures occurred in some panel nodes whereas the bending damage it is confined to the masonry walls. Concerning the shear damage, it is attained in North and South façades, respectively. In terms of ductility (μ), in X direction the estimated value is 2,87 to which correspond to an increase of 16,7% compared to the ductility calculated in the Y direction, equal to 2,4.

The estimated vulnerability indices associated with the two main directions X and Y are evaluated as the ratio between the seismic demand and the corresponding capacity of the building considering the Ultimate Limite State (ULS). In particular, the calculated indexes, in X and Y direction, are 0,38 and 0,48, respectively.

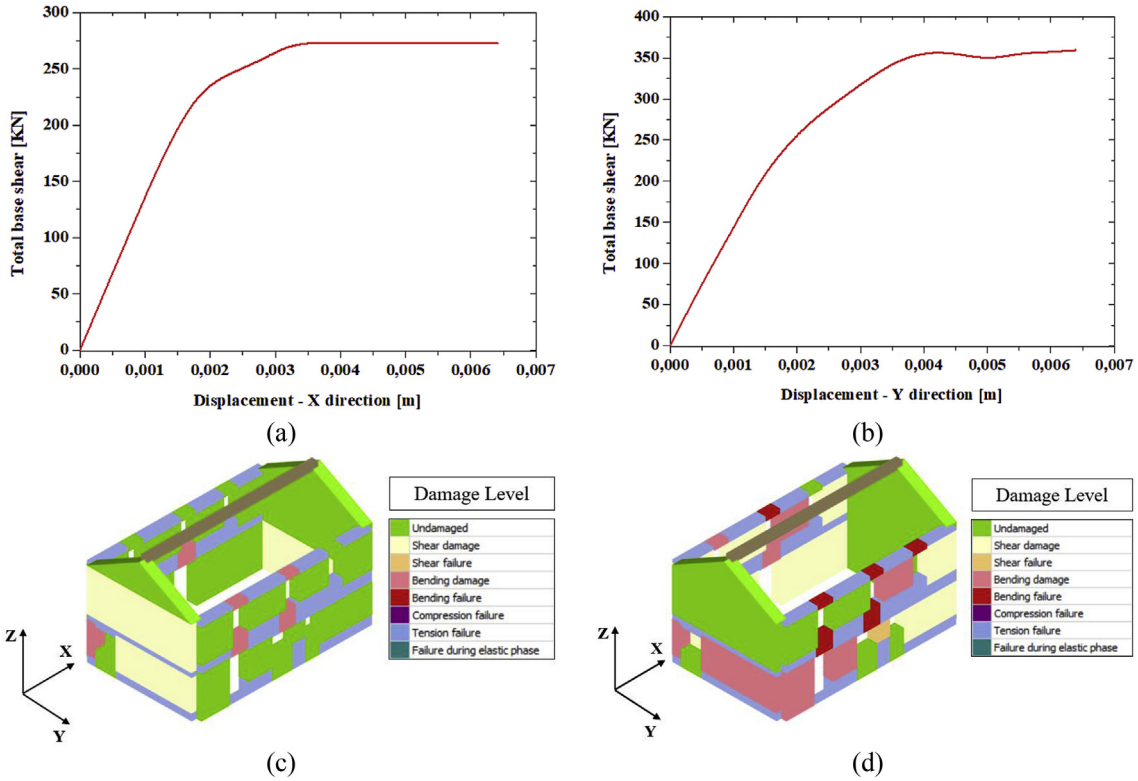

Fig. 17. SdoF capacity curves: (a) X direction, (b) Y direction, (c) damage level in X direction and (d) damage level in Y direction.

Table 5
Damage thresholds.

Damage Limit State, D_i		Displacement Limit State
D_1	Slight	0,7 D_y
D_2	Moderate	D_y
D_3	Near collapse	D_y +0,5(D_u - D_y)
D_4-D_5	Collapse	D_u

Table 6
Standard deviation for each damage thresholds.

Standard Deviation, β_i		Ductility Limit State
β_1	Slight	0,25 + 0,07ln(μ)
β_2	Moderate	0,2 + 0,18ln(μ)
β_3	Near collapse	0,1 + 0,41ln(μ)
β_4-β_5	Collapse	0,15 + 0,5ln(μ)

5.3. Mechanical fragility curves

Fragility curves express the probability of exceeding a generic damage threshold, D_K, for a predetermined value of the Intensity Measurement (*IM*), generally represented by the PGA or spectral displacements, S_d. The evaluation of the fragility curves is carried out according to the methodology proposed by Ref. [4]. In particular, four damage thresholds, D1 (slight), D2 (moderate), D3 (near collapse) and D4-D5 (collapse), have been defined and achieved in Table 5. As can be seen, the damage states are intrinsically defined considering the yielding displacement (D_y) and ultimate displacement (D_u) of the SDoF system.

Methodologically, fragility curves are defined according to Equation (6)

$$P[D_K|PGA] = \Phi\left[\frac{1}{\beta}\cdot\left(\frac{PGA}{PGA_{D_K}}\right)\right] \quad (6)$$

where, Φ, is the cumulative distribution function, PGA_{DK} is the median acceleration value associated for each damage threshold and β is the standard deviation of the log-normal distribution.

The dispersion, β, generally depends on the contribution of uncertainties in the seismic demand. This parameter is a function of the ductility, μ, of the structural system intended as the ratio between ultimate displacement, D_u, and the corresponding yielding displacement, D_y. Based on this assumption, the estimated value of the dispersions is given in Table 6 [42].

However, in this research work, the proposed fragility functions are derived according to Equation (7)

$$S_{a,e} = \omega^2 \cdot S_{d,e} = \left(\frac{2\cdot\pi}{T}\right)^2 \cdot S_{D_K} \quad (7)$$

where S_{ae} is the expected spectral acceleration, T is the vibration period of the structural system and S_{DK} is the spectral displacement associated with the damage thresholds reported in Table 4. Therefore, the fragility curves have been plotted in both directions, longitudinal X and transversal Y, respectively, and depicted in Fig. 18.

Accordingly, it has been possible to compare the fragility functions for the assessment methods proposed in the present work. The gotten results are depicted in Fig. 19.

From the comparison of the applied methodologies, it has been possible to notice how the fragility curves present different values of the expected damage. Generally, this discrepancy is due to the different procedures to estimate the damage threshold, D_K, and the uncertainties, β_i.

From one side, the macroseismic methodology, used for large-scale assessment, adopts an acceleration-intensity conversion law for the identification of the PGA range and, subsequently, it allows to plot the fragility curves through the cumulative distribution function regardless of the uncertainties, β. On the other hand, the mechanical procedure provides more refined results since it takes into account the uncertainties of the structural system and combines them through the lognormal distribution.

Nevertheless, the macroseismic method in both analysis directions tends to overestimate the damage thresholds D1 and D2 by 5% and 10%, respectively, for a spectral acceleration enclosed in the range [0 ÷ 0,3 g]. Contrary, for PGA values greater than 0,3 g, this method provides an underestimation for each damage levels considered. In particular, considering a damage D4 and D5 in both directions, it is possible to estimate a mean percentage decrease of 30% and 20%, compared to the mechanical procedure. Hence, the analytical method employed in this study may be used in constructing the fragility curves since it provides more refined results than the curves calibrated on the empirical-macroseismic method that can not introduce various structural parameters and also, they require a large amount of damage data.

6. Conclusion

The study illustrates a comparison between two different approaches for estimating seismic vulnerability in terms of expected damage for an isolated masonry building located in the centre of Muccia. The study area was composed of 50 structural units erected in aggregate, opportunely classified according to the BTM in three different classes as M3.1, M3.3, and M3.4, respectively.

The assessment of the seismic vulnerability of the inspected urban-sector has been analysed by means of the index method approach. The statistical distribution of vulnerability indices shows, globally, a

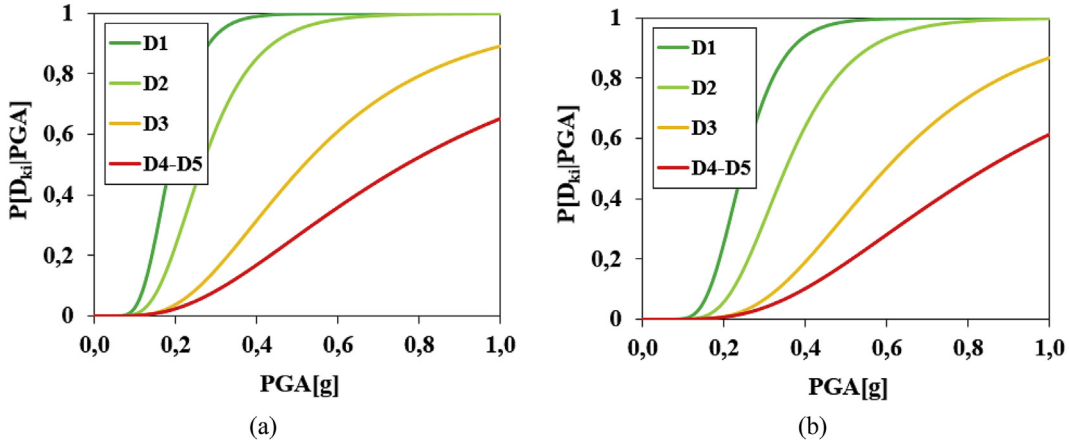

Fig. 18. Fragility curves (a) X direction, (b) Y direction, respectively.

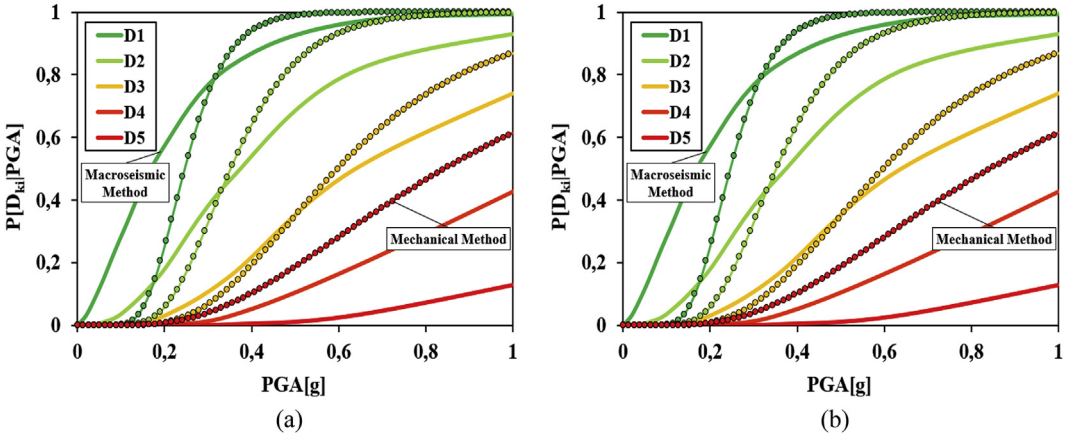

Fig. 19. Fragility curves comparison (a) X direction, (b) Y direction.

medium vulnerability of the stock.

Afterward, mean typological vulnerability curves were derived in order to characterise the expected global damage varying the macroseismic intensity according to the EMS-98 scale. The gotten results showed that, for seismic intensities less than X grade, the expected damage has not been relevant, but for high values of seismic intensity ($X < I_{EMS\text{-}98} < XII$), the expected damage would cause an incipient collapse of the analysed sample.

Analysis of the damage scenario by means parametric approach have been considered using the attenuation law in terms of seismic intensity proposed by Crespellani.

Having defined a set of occurred magnitude (M_w) and site-source distances (R), it has been possible to analyse in detail the influence of these factors on an urban scale. The results obtained have shown that the most severe scenario was for $M_w = 6,5$ in which at least 40% of the buildings reached damage D2 (Substantial damage) and 8% of the cases reached damage D4 (Extended damage).

Subsequently, an isolated building was considered as a case study. The mechanical approach was used for the characterisation of the structural model. A macro-element model of the historical building has been set-up through a mesh of masonry piers and spandrels. The capacity of the structure in the *Y* direction has shown higher damage than the orthogonal ones. In fact, considering a failure hierarchy a bending and shear damages tend to increase globally. In terms of ductility (μ), the results achieved shown an estimated value of $\mu = 2,87$ in the X direction which corresponds to a percentage increment of 16,7% compared to the ductility calculated in the other direction and equal to 2,4. The vulnerability indexes in both analysis directions, X and Y, are evaluated as the ratio between the seismic demand and the capacity of the structure. The estimated values were 0,38 and 0,48 respectively.

Consecutively, the fragility curves have been derived for both, empirical and mechanical approaches. From the comparison of the applied methodologies, the fragility curves present different values of the expected damage since they are based on different procedures to estimate the damage threshold, D_K, and the uncertainties, β_i. In particular, the macroseismic method in both analysis directions tends to overestimate the damage thresholds by 5% and 10%, respectively, for a spectral acceleration enclosed in the range [0 ÷ 0,3 g].

Contrary, for PGA values greater than 0,3 g, this method provides an underestimation for each damage levels considered of 30% and 20%, compared to the mechanical procedure. In conclusion, the macroseismic method can be considered an exhaustive approach for urban scale scenario analysis but its empirical nature tends to underestimate the damage compared to the mechanical ones. To improve the fragility curves it will, therefore, be necessary to improve the estimation of the exposure at the time of the earthquake and to complete the observational database in order to ensure all the information on the surveyed buildings can be processed. For these reasons, the mechanical methodology used for estimating the expected damage through fragility curves is a proven reliability method for the evaluation of seismic vulnerability.

Appendix A. Supplementary data

Supplementary data to this article can be found online at https://doi.org/10.1016/j.jobe.2019.100813.

References

[1] O.D. Cardona, M.K. van Aalst, J. Birkmann, M. Fordham, G. McGregor, R. Perez, R.S. Pulwarty, E.L.F. Schipper, B.T. Sinh, Determinants of Risk : Exposure and Vulnerability Coordinating, Managing the Risks of Extreme Events and Disasters to Advance Climate Change Adaptation, (2012), https://doi.org/10.1017/CBO9781139177245.005.

[2] A.H. Barbat, M.L. Carreño, L.G. Pujades, N. Lantada, O.D. Cardona, M.C. Marulanda, Seismic Vulnerability and Risk Evaluation Methods for Urban Areas. A Review with Application to a Pilot Area, Structure and Infrastructure Engineering, 2010, https://doi.org/10.1080/15732470802663763.

[3] R. Gonzalez-Drigo, A. Avila-Haro, A.H. Barbat, L.G. Pujades, Y.F. Vargas, S. Lagomarsino, S. Cattari, Modernist unreinforced masonry (URM) buildings of barcelona: Seismic vulnerability and risk assessment, Int. J. Archit. Herit. (2015), https://doi.org/10.1080/15583058.2013.766779.

[4] P. Lamego, P.B. Lourenço, M.L. Sousa, R. Marques, Seismic vulnerability and risk analysis of the old building stock at urban scale: Application to a neighbourhood in Lisbon, Bull. Earthq. Eng. 15 (2017) 2901–2937, https://doi.org/10.1007/s10518-016-0072-8.

[5] P.B. Lourenço, J.A. Roque, Simplified indexes for the seismic vulnerability of ancient masonry buildings, Constr. Build. Mater. (2006), https://doi.org/10.1016/j.conbuildmat.2005.08.027.

[6] M.P. Ciocci, S. Sharma, P.B. Lourenço, Engineering simulations of a super-complex cultural heritage building: Ica Cathedral in Peru, Meccanica (2018), https://doi.org/10.1007/s11012-017-0720-3.

[7] M. Angelillo, P.B. Lourenço, G. Milani, Masonry behaviour and modelling, CISM International Centre for Mechanical Sciences, Courses and Lectures, 2014, , https://doi.org/10.1007/978-3-7091-1774-3_1.

[8] S. Tiberti, G. Milani, Historic city centers after destructive seismic events, the case of finale Emilia during the 2012 Emilia-Romagna earthquake: Advanced numerical modelling on four case studies, Open Civ. Eng. J. (2017), https://doi.org/10.2174/1874149501711011059.

[9] S. Lagomarsino, S. Giovinazzi, Macroseismic and mechanical models for the vulnerability and damage assessment of current buildings, Bull. Earthq. Eng. (2006), https://doi.org/10.1007/s10518-006-9024-z.

[10] S. Cara, A. Aprile, L. Pelà, P. Roca, Seismic Risk Assessment and Mitigation at Emergency Limit Condition of Historical Buildings along Strategic Urban Roadways. Application to the “Antiga Esquerra de L’Eixample” Neighborhood of Barcelona, Int. J. Archit. Herit. 12 (2018) 1055–1075, https://doi.org/10.1080/15583058.2018.1503376.

[11] F. Clementi, E. Quagliarini, F. Monni, E. Giordano, S. Lenci, Cultural heritage and earthquake: The case study of in Ascoli Piceno, Open Civ. Eng. J. (2017), https://doi.org/10.2174/1874149501711011079.

[12] F. Clementi, V. Gazzani, M. Poiani, S. Lenci, Assessment of seismic behaviour of heritage masonry buildings using numerical modelling, J. Build. Eng. (2016), https://doi.org/10.1016/j.jobe.2016.09.005.

[13] M. Valente, G. Milani, E. Grande, A. Formisano, Historical masonry building aggregates: Advanced numerical insight for an effective seismic assessment on two

row housing compounds, Eng. Struct. 190 (2019) 360–379.
[14] S. Tiberti, M. Acito, M. Milani, Comprehensive FE numerical insight into Finale Emilia Castle behaviour under 2012 Emilia Romagna seismic sequence: Damage causes and seismic vulnerability mitigation hypothesis, Eng. Struct. 117 (2016) 397–421.
[15] M. Valente, G. Milani, Damage assessment and collapse investigation of three historical masonry palaces under seismic actions, Eng. Fail. Anal. 98 (2019) 10–37.
[16] T.M. Ferreira, R. Maio, R. Vicente, Seismic vulnerability assessment of the old city centre of Horta, Azores: Calibration and application of a seismic vulnerability index method, Bull. Earthq. Eng. (2017), https://doi.org/10.1007/s10518-016-0071-9.
[17] A. Basaglia, A. Aprile, E. Spacone, F. Pilla, Performance-based seismic risk assessment of urban systems, Int. J. Archit. Herit. 12 (2018) 1131–1149, https://doi.org/10.1080/15583058.2018.1503371.
[18] G. Grünthal (Ed.), Chaiers du Centre Européen de Géodynamique et de Séismologie: Volume 15-European Macroseismic Scale 1998, European Center for Geodynamics and Seismology, Luxembourg, 2879770084, 1998.
[19] D. Rapone, G. Brando, E. Spacone, G. De Matteis, Seismic vulnerability assessment of historic centers: Description of a predictive method and application to the case study of scanno (Abruzzi, Italy), Int. J. Archit. Herit. 12 (2018) 1171–1195, https://doi.org/10.1080/15583058.2018.1503373.
[20] Savini Patrizio, Storia della città di Camerino, Second, Tipografia Sarli, 1864.
[21] L. Chiaraluce, R. Di Stefano, E. Tinti, L. Scognamiglio, M. Michele, E. Casarotti, M. Cattaneo, P. De Gori, C. Chiarabba, G. Monachesi, A. Lombardi, L. Valoroso, D. Latorre, S. Marzorati, The 2016 Central Italy seismic sequence: A first look at the mainshocks, aftershocks, and source models, Seismol Res. Lett. (2017), https://doi.org/10.1785/0220160221.
[22] INGV, Rapporto Di Sintesi Sul Terremoto in Centro Italia Mw 6.5 del 30 Ottobre 2016, Gruppo Di Lavoro INGV Sul Terremoto in Centro Italia, (2016), pp. 1–49, https://doi.org/10.5281/zenodo.166019.
[23] National Institute of Geophysics and Vulcanology, Prime interpretazioni dall'interferogramma differenziale ottenuto da dati radat del satellite europeo Sentinel-1, (2016) https://ingvterremoti.wordpress.com.
[24] P. Mouroux, B. Le Brun, Presentation of RISK-UE project, Bull. Earthq. Eng. (2006), https://doi.org/10.1007/s10518-006-9020-3.
[25] A. Formisano, G. Florio, R. Landolfo, F.M. Mazzolani, Numerical calibration of an easy method for seismic behaviour assessment on large scale of masonry building aggregates, Adv. Eng. Software (2015), https://doi.org/10.1016/j.advengsoft.2014.09.013.
[26] N. Chieffo, A. Formisano, Geo-hazard-based approach for the estimation of seismic vulnerability and damage scenarios of the old city of Senerchia (Avellino, Italy), Geosciences 9 (2019) 59, https://doi.org/10.3390/geosciences9020059.
[27] N. Chieffo, A. Formisano, The influence of geo-hazard effects on the physical vulnerability assessment of the built heritage: An application in a district of Naples, Buildings 9 (2019) 26, https://doi.org/10.3390/buildings9010026.
[28] D. Benedetti, V. Petrini, Sulla vulnerabilità si sismica di edifici in muratura: Un metodo di valutazione, L'Industria Delle Costruzioni, 1984.
[29] N. Chieffo, A. Formisano, T.M. Ferreira, Damage scenario-based approach and retrofitting strategies for seismic risk mitigation: An application to the historical Centre of Sant'Antimo (Italy), Eur. J. Environ. Civ. Eng. 0 (2019) 1–20, https://doi.org/10.1080/19648189.2019.1596164.
[30] S. Lagomarsino, On the vulnerability assessment of monumental buildings, Bull. Earthq. Eng. 4 (4) (2006) 445–463, https://doi.org/10.1007/s10518-006-9025-y.
[31] T.M. Ferreira, R. Vicente, H. Varum, Seismic Vulnerability Assessment of Masonry Facade Walls: Development, Application and Validation of a New Scoring Method, Structural Engineering and Mechanics, (2014), https://doi.org/10.12989/sem.2014.50.4.541.
[32] R. Vicente, T.M. Ferreira, R. Maio, Seismic risk at the urban scale: Assessment, mapping and Planning, Procedia Econ. Finance 18 (2014) 71–80, https://doi.org/10.1016/S2212-5671(14)00915-0.
[33] T. Crespellani, C.A. Garzonio, Seismic risk assessment for the preservation of historical buildings in the city of Gubbio, Geotechnical Engineering for the Preservation of Monuments and Historic Sites: Proceedings of the International Symposium on Geotechnical Engineering for the Preservation of Monuments and Historic Sites, 1997 Napoli, Italy, 3-4 October 1996.
[34] E. Guagenti, V. Petrini, The case of old buildings: Towards a new law - Intensity damage, Proceedings of the 12th Italian Conference on Earthquake Engineering—ANIDIS, Italian National Association of Earthquake Engineering, Pisa, Italy, 1989, , https://doi.org/10.1017/CBO9781107415324.004 (in Italian)..
[35] DM 17/01/2018, Aggiornamento delle "Norme Tecniche per le Costruzioni" - NTC 2018, (2018), pp. 1–198.
[36] S.T.A data srl, 3Muri 10.9.0 - User Manual, (n.d.).
[37] E. Quaglierini, G. Maracchini, F. Clementi, Uses and limits of the equivalent frame model on existing unreinforced masonry buildings for assessing their seismic risk: A review, J. Build. Eng. (2017), https://doi.org/10.1016/j.jobe.2017.03.004.
[38] A. Formisano, Theoretical and numerical seismic analysis of masonry building aggregates: Case studies in san Pio Delle Camere (L'Aquila, Italy), J. Earthq. Eng. (2017), https://doi.org/10.1080/13632469.2016.1172376.
[39] A. Formisano, Local- and global-scale seismic analyses of historical masonry compounds in San Pio delle Camere (L'Aquila, Italy), Nat. Hazards (2017), https://doi.org/10.1007/s11069-016-2694-1.
[40] F. Clementi, A. Pierdicca, A. Formisano, F. Catinari, S. Lenci, Numerical model upgrading of a historical masonry building damaged during the 2016 Italian earthquakes: The case study of the Podestà palace in Montelupone (Italy), J. Civ. Struct. Health Monit. 7 (2017) 703–717, https://doi.org/10.1007/s13349-017-0253-4.
[41] Eurocode 8, European Standard EN 1998-3:2005: Design of Structures for Earthquake Resistance - Part 3: Assessment and Retrofitting of Buildings, Comite Europeen de Normalisation, Brussels, 2005.
[42] Z.V. Milutinovic, G.S. Trendafiloski, WP4:Vulnerability of Current Buildings. Risk-UE Project Handbook, European Comission, 2003, https://doi.org/10.1007/978-1-4020-3608-8_23.